The Reactivity of Tungsten Hexachloride with Tetrahydrofuran and 2-Methoxyethanol

Sabrina Bianchi [a], Marco Bortoluzzi [b], Valter Castelvetro [a], Fabio Marchetti [a,*],

Guido Pampaloni [a], Calogero Pinzino [c], Stefano Zacchini [d]

[a] *Università di Pisa, Dipartimento di Chimica e Chimica Industriale, Via Moruzzi 13, I-56124 Pisa, Italy*

[b] *Ca' Foscari Università di Venezia, Dipartimento di Scienze Molecolari e Nanosistemi, Via Torino 155, I-30175 Mestre (Venezia), Italy.*

[c] *ICCOM-CNR UOS Pisa, Research Area, Via Moruzzi 1, I-56124 Pisa, Italy.*

[d] *Dipartimento di Chimica Industriale "Toso Montanari", Università di Bologna, Viale Risorgimento 4, I-40136 Bologna, Italy*

---

* Corresponding author. Tel.: +390502219245; Webpage: http://www.dcci.unipi.it/fabio-marchetti.html.

E-mail address: fabio.marchetti1974@unipi.it

Abstract

The ring opening polymerization reaction of tetrahydrofuran (thf) by WCl_6 was investigated under different conditions, and the polymeric material was characterized by NMR and SEC (Size Exclusion Chromatography) analyses. The mixed valence complex $[(thf)_2(\mu-H)][\{WOCl_3(thf)\}_2(\mu-O)]$, **3**, was isolated from the reactions of WCl_6 with 4-8 equivalents of thf in dichloromethane at room temperature, and crystallographically characterized. The formation of **3** was preceded by that of $WOCl_4(thf)$, **2**, while $Cl(CH_2)_4Cl$ and $Cl(CH_2)_4O(CH_2)_4Cl$ were identified as the prevalent organic side products. The 1:1 molar reaction of WCl_6 with $MeO(CH_2)_2OH$, in CH_2Cl_2 at room temperature, afforded the dinuclear complexes $(WOCl_4)_2(\mu-\kappa^2-1,4-dioxane)$, **4**, and $WCl_5(OCH_2CH_2OMe)$, **5**, in admixture with $Cl(CH_2)_2Cl$, $MeO(CH_2)_2OMe$ and MeCl. Also complex **4**, resulting from a C−O bond forming process, was characterized by X-ray crystallography.

Keywords: Tungsten hexachloride, Tetrahydrofuran, 2-methoxyethanol, Ring Opening Polymerization, C−O cleavage

1. Introduction

Tungsten hexachloride, WCl_6, is an easily accessible Lewis acidic, strongly oxophilic species, which is capable of promoting the activation of different classes of oxygen containing organic compounds [1]. In general, two main reaction pathways may be working when WCl_6 is allowed to contact with an oxygen donor, i.e. the chlorine/oxygen intermolecular exchange [2, 3], and the metal reduction to W(V) or W(IV) species [2c, 3c, 4]. These reduction pathways may be accompanied by the release of elemental chlorine [2c, 4d], otherwise the organic counterpart behaves as electron transfer source in some cases [4a, 5].

We recently described the reactions of WCl_6 with limited amounts of aliphatic and aryl-ethers [6]. Cyclic ethers and WCl_6 reversibly form heptacoordinated complexes in solution, i.e. $WCl_6(L)$ (L = 1,4-dioxane or tetrahydropyran), and the weak adduct containing tetrahydropyran undergoes Cl/O interchange process at high temperature [6a]. In general, when WCl_6-promoted ether activation is working, it usually proceeds with the cleavage of either one or two C−O bonds, thus affording metal-alkoxide and metal-oxide species, respectively. This feature is in agreement with the generally observed activation of ethers by high valent transition metal chlorides [7]. Otherwise, the coupling of fragments and, in particular, the formation of new C−O bonds is commonly not favored, an exception being the MCl_5 (M = Nb, Ta) directed generation of dioxanes from 1,2-dialkoxyalkanes [8].

As a strong Lewis acid, WCl_6 is known to promote the cationic ring opening polymerization of tetrahydrofuran [9], and possible optimized reaction conditions were established in order to maximize monomer conversion and polymer molecular weight [9b]. Furthermore, $WOCl_3(thf)_2$ was claimed to be prepared by the addition of ca. 10 equivalents of thf to WCl_6 in cyclohexane, and then used as a starting material to access $WOCl_3$ derivatives [10]. This reaction was described to be very sensitive to the conditions (solvent, time, etc.) and to the scale.

In the framework of our exploration on the chemistry of high valent transition metal halides, herein we supply more details on the reactivity of WCl_6 with thf, including the molecular weight characterization by SEC (Size Exclusion Chromatography) of the polymeric materials obtained under different conditions, and the crystallographic characterization of an ionic complex possibly involved in the polymer chain growth. The study has been extended to the reaction of WCl_6 with 2-methoxyethanol, $MeO(CH_2)_2OH$, i.e. a molecule comprising both an ether function and an alcoholic one. Studies on the reactivity of WCl_6 with alkoxy-ethers are lacking in the literature, while it is well established that the reactions of alcohols with high valent transition metal chlorides in general [11], and WCl_6 in particular [11c, d], represents a

3

convenient strategy to access metal alkoxides.

In the reaction of WCl$_6$ with MeO(CH$_2$)$_2$OH, the cleavage of C−O bonds is partially accompanied by the formation of new C−O bonds, and this has been unambiguously ascertained by a X-ray diffraction study.

2. Results and Discussion

2.1. Reactivity of WCl$_6$ with tetrahydrofuran.

Poly(tetrahydrofuran) was generated by WCl$_6$ under different experimental conditions (reaction time, temperature). The reaction yields and the molecular weight values of the resulting polymer materials are reported in Table 1, while the corresponding molecular weight distribution derived from the SEC traces are shown in Figure 1. In accordance with previous findings, a higher monomer conversion was achieved at 0 °C rather than at room temperature [9b].

Table 1. Number- ($\overline{M}_n$) and weight-average ($\overline{M}_w$) molecular weights and polydispersity index ($\overline{M}_w/\overline{M}_n$) for the polymers obtained under different reaction conditions, as determined by SEC in thf.

Run	T (°C)	t (h)	Yield (%)	$\overline{M}_n$ [a] (g·mol^{-1})	$\overline{M}_w$ [a] (g·mol^{-1})	
A	20	8	36	11037	24656	2.23
B	20	18	17	7784	31374	4.03
C	0	8	70	2727	17358	6.36

[a] Molecular weight data relative to a poly(styrene) standards calibration curve. Since the Flory-Huggins polymer-solvent interaction parameter for thf with poly(styrene) and poly(thf), respectively, are quite close [12], the polymer coil expansion and hydrodynamic volume in solution should be similar. Thus the obtained values should match well the actual (absolute) molecular weights.
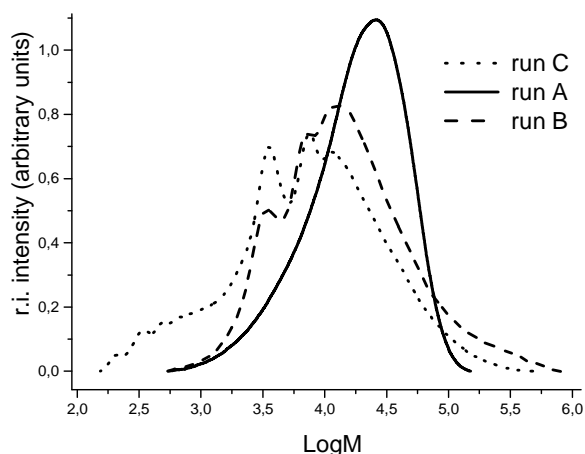
Figure 1. Molecular weight distribution of poly(tetrahydrofuran) from SEC analysis in thf, based on a poly(styrene) calibration curve.

In order to isolate and/or detect possible intermediates/by-products along the polymerization process, the reactions of WCl_6 with controlled amounts of thf were carried out in dichloromethane, i.e. a widely considered non coordinating solvent [13]. The interaction of WCl_6 with thf presumably starts with the formation of the weak adduct $WCl_6(thf)$, **1**, for which DFT calculations ruled out the alternative, ionic structure $[WCl_5(thf)]Cl$, which was calculated as being less stable by about 18.2 kcal mol^{-1} (Gibbs free energy). Indeed, similar WCl_6L complexes were previously identified as initial products of the interaction of WCl_6 with other cyclic ethers, see Introduction [6a]. In the present case, NMR experiments failed to detect **1**, probably in view of the highly favorable, subsequent activation of the thf ligand (Eqn. 1). Figure 2 reports the DFT-optimized structure of **1**. It can be described in terms of a distorted monocapped trigonal prism comprising six similar W−Cl bonds and a single W−O bond. Interestingly, the computed W−O distance is 2.428 Å in **1**, whereas it is around 2.9 - 3.0 Å in the homologous complexes containing a six-membered O-donor heterocycle [6a].

5
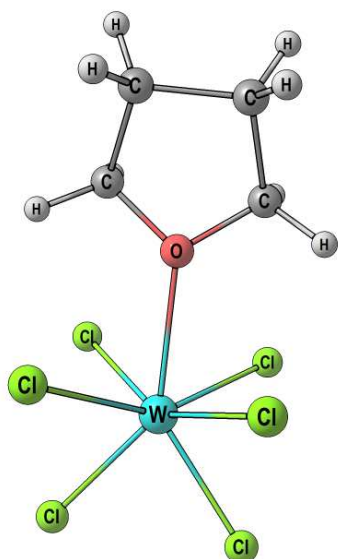
Figure 2. DFT C-PCM/ωB97X calculated structure of WCl$_6$(thf), **1**. Dichloromethane as implicit solvent. Selected computed bond lengths (Å) and angles (°) are: W−O 2.428, W−Cl 2.340, 2.340, 2.343, 2.349, 2.349, 2.354, O−W−Cl 72.6, 73.5, 74.2, 74.7, 141.3, 142.0.

The 1:2 molar reaction WCl$_6$/thf led to the high yield isolation of WOCl$_4$(thf), **2**, as a result of Cl/O interchange between the metal centre and one equivalent of organic reactant, followed by metal coordination of the second equivalent. Accordingly, a NMR experiment indicated the clean formation of 1,4-dichlorobutane (Eqn. 1 and Scheme 1).

$$WCl_6 + 2\ thf \rightarrow \underset{\mathbf{2}}{WOCl_4(thf)} + Cl(CH_2)_4Cl \qquad \Delta G = -49.3\ \text{kcal mol}^{-1} \qquad (1)$$

Compound **2** could be obtained also by the 1:1 molar combination of WOCl$_4$ with thf [14]. The calculated structure of **2** is shown in Figure 3: it closely resembles that reported for the W(V) anion [WOCl$_4$(THF)]⁻ [15]. The computed W=O bond, 1.665 Å, is only slightly shorter than the experimental value of 1.692(8) Å. The W−O(THF) distances are yet more similar, i.e. 2.351 Å in the DFT-optimized geometry and 2.358(7) in [WOCl$_4$(THF)]⁻. In both the cases, the O−W−O angle is close to 180° [179.9° in the W(VI) derivative and 179.7(4) in the W(V) one]. The W−Cl bond lengths are also comparable, the average values being 2.337 Å (DFT) and 2.358 Å (X-ray). In both the cases, the W centre is moved away from the least square

6

plane described by the chlorine atoms, and the O=W−Cl angles are between 95 and 99°. The root-mean-square deviation of atomic positions, on considering the metal centre and the atoms in the first coordination sphere, is very low (0.047 Å). The comparison of computed and experimental data suggests that the change of configuration from d^0 to d^1 scarcely influences the nature of the interactions of the metal centre with the ligands.
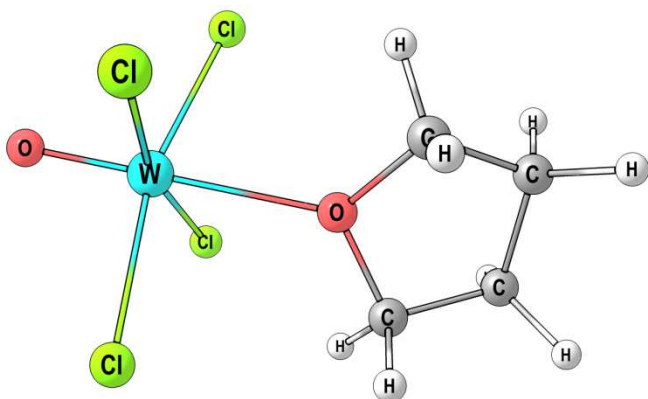
Figure 3. DFT C-PCM/ωB97X calculated structure of WOCl₄(thf), **2**. Dichloromethane as implicit solvent. Selected computed bond lengths (Å) and angles (°) are: W=O 1.665, W-O 2.351, W-Cl 2.325, 2.325, 2.327, 2.372, O=W-O 179.9, O=W-Cl 97.9, 97.9, 98.2, 98.2.

The IR spectrum (solid state) of **2** displays a diagnostic, intense band at 999 cm^{-1}, ascribable to the W=O moiety [2a,c, 16]. The NMR spectra (in CD$_2$Cl$_2$) exhibit the typical thf pattern, the resonances being low field shifted with respect to non coordinated thf.

The reactions of WCl$_6$ with a four to eight fold excess of thf, at room temperature, afforded dark-green/blue solutions [10]; several attempts of crystallization were performed by layering directly the reaction solutions with hexane in a Schlenk tube, and all of the attempts provided some green crystals of [(thf)$_2$(μ-H)][{WOCl$_3$(thf)}$_2$(μ-O)], **3**. The molecular structure was ascertained by a X-ray diffraction study (Figure 4 and Table 2). **3** is an ionic compound, comprising mixed valence, formally W(V)-W(VI), anions. Each cation is composed by a protonated thf forming a strong asymmetric H-bond with a second thf unit [O(7)–H(7) 0.90(2) Å, H(7)···O(6) 1.50(2) Å, O(7)···O(6) 2.353(14) Å, <O(7)H(7)O(6) 156(7)°] [17]. The H(7) proton bonded to O(7) was located in the Fourier map and refined consequently.

The structure of the anion can be described in terms of two $WO_2Cl_3(thf)$ octahedra sharing a bridging oxide ligand. The two W centers display distorted octahedral geometries (with the W atoms moved 0.299 and 0.291 Å away from, respectively, the least square planes described by the three Cl and the μ-O ligands), the same chemical environment and very similar bonding parameters, as previously found in other mixed W(VI)-W(V) oxide chloride anions [18]. Around each metal centre, the thf ligand is *trans* to the terminal oxide, while the O(1) and O(2) terminal oxide ligands bonded to W(1) and W(2), respectively, are in relative *pseudo-trans* position. Likewise W(1)−O(1) [1.678(11) Å] and W(2)−O(2) [1.685(11) Å], also the W(1)–O(3) [1.868(12) Å] and W(2)–O(3) [1.884(12) Å] distances involving the bridging O(3) ligand are rather short. This indicates some π character in the W−O−W bridge, as also suggested by the W(1)−O(3)−W(2) angle [177.1(6)°], being very close to linearity [18, 19]. The π-character of the linear W(1)−O(3)−W(2) chain allows an easy electronic exchange between two neighboring tungsten atoms.

8
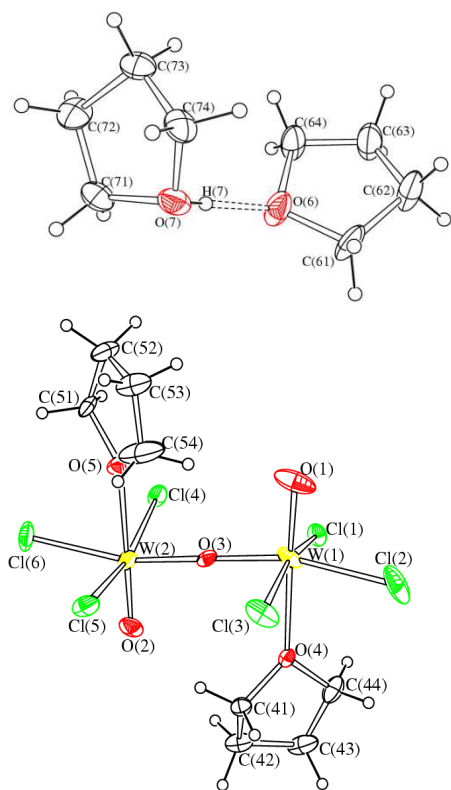
Figure 4. View of the molecular structure of [(thf)$_2$(μ-H)][{WOCl$_3$(thf)}$_2$(μ-O)], **3**, with key atoms labeled. Displacement ellipsoids are at the 50% probability level. The H-bond in the [(thf)$_2$(μ-H)]$^+$ cation is represented as a dashed line.

Table 2. Selected bond lengths (Å) and angles (°) for **3**

W(1)–O(1)	1.678(11)	W(2)–O(2)	1.685(11)
W(1)–O(3)	1.868(12)	W(2)–O(3)	1.884(12)
W(1)–O(4)	2.289(9)	W(2)–O(5)	2.293(11)
W(1)–Cl(1)	2.365(3)	W(2)–Cl(5)	2.359(4)
W(1)–Cl(3)	2.358(3)	W(2)–Cl(4)	2.361(3)
W(1)–Cl(2)	2.362(5)	W(2)–Cl(6)	2.376(4)
Cl(1)–W(1)–Cl(3)	164.15(12)	Cl(4)–W(2)–Cl(5)	165.74(13)
O(1)–W(1)–O(4)	179.4(5)	O(2)–W(2)–O(5)	179.4(5)
O(3)–W(1)–Cl(2)	164.9(3)	O(3)–W(2)–Cl(6)	163.8(4)
O(1)–W(1)–O(3)	99.8(7)	O(2)–W(2)–O(3)	99.3(5)
W(1)–O(3)–W(2)	177.1(6)		

In the IR spectrum of **3** (solid state), the [W=O] band has been found at 983 cm^{-1}. The EPR spectrum (in CH$_2$Cl$_2$, Figure 5) well matches the computed spectrum (experimental g$_{iso}$ = 1.77461, linewidth = 94.48 G [20]; calculated parameters: g$_{//}$ = 1.78842, g$_\perp$ = 1.77457, g$_{iso}$ = 1.77919). The calculated structure and the spin density distribution of **3** indicate that the electron spin density is equally distributed on the two W atoms, each of them in a +5.5 average oxidation state (Figure 6).
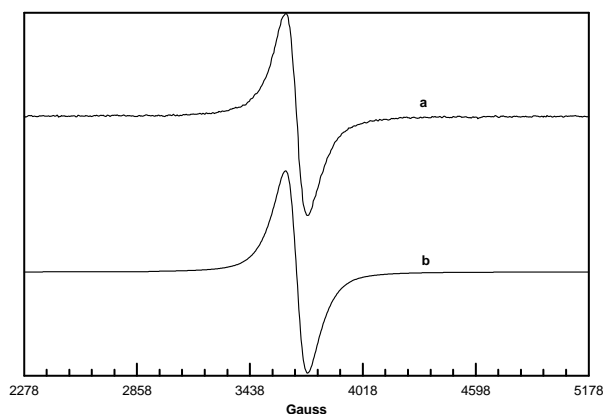
Figure 5. Experimental (a) and calculated (b) EPR spectra (CH$_2$Cl$_2$, 298 K) of [(thf)$_2$(μ-H)][{WOCl$_3$(thf)}$_2$(μ-O)], **3**.

The spin density of the molecule is mainly attributable to the electron occupying the α-HOMO molecular orbital (ε = −7.47 eV), showing essentially non-bonding character (Figure 6). The α-HOMO is 2.30 eV higher in energy with respect to the β-HOMO, and 1.32 eV

9

lower than the first unoccupied MO (α-LUMO). The overall MO diagram is represented in

Figure 7.
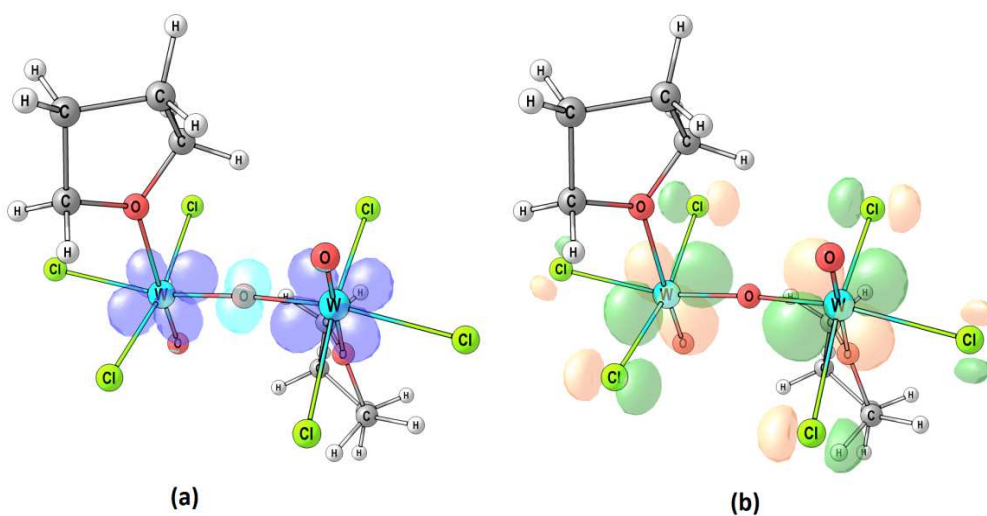
Figure 6. DFT C-PCM/ωB97X calculated structure of [(thf)$_2$(μ-H)][{WOCl$_3$(thf)}$_2$(μ-O)], **3**. Dichloromethane as implicit solvent. (a) Spin density surface, isovalue = 0.01 a.u. (b) α-HOMO, surface isovalue = 0.05 a.u. Selected computed bond lengths (Å) and angles (°):W=O (*terminal*) 1.677, W=O (*bridging*) 1.877, W−O (*thf*) 2.376, W−Cl (*trans Cl*) 2.379, W−Cl (*trans O*) 2.401, O(*terminal*)−W−O(*thf*) 178.1, O(*terminal*)−W−O(*bridging*) 99.8, O(*terminal*)−W−Cl 96.7, 98.9, 99.0, W−O−W 175.1.
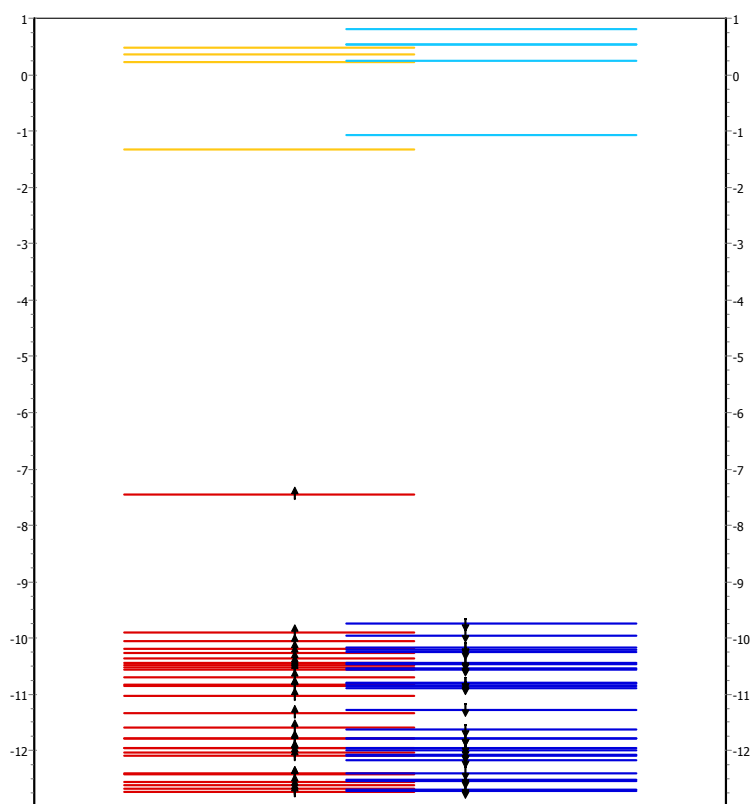
DFT calculations allowed comparison of the three different W−O bond types in **3** by means of Mayer analysis. As expected, the interactions with the terminal oxo-ligands resulted the strongest ones, the bond order being around 2.27. The computed bond order between the W centers and μ-O is about 0.95, while the bond order with the thf ligands is 0.28.

In principle, the formation of the cationic part of **3**, containing a proton, could result from different sources, including the hardly avoidable presence of traces of water in the reaction medium. It should be noted that the NMR analysis on a CD_2Cl_2 reaction mixture (thf/W ratio = 4), in a sealed NMR tube, suggested the presence of traces of 1,3-butadiene. The possible formation of 1,3-butadiene from thf dehydration by early transition metal compounds was previously ascertained, and might contribute here to the formation of **3** [21].

In order to shed light on mechanistic aspects related to the polymerization process, we performed a series of analytical and spectroscopic studies.

According to conductivity measurements (see Experimental), it is likely that ionic species, including **3**, play some role during the polymerization process. In particular, the protonated thf moiety in **3** could act directly or indirectly as the initiating species for the growth of the polymer chain via sequential thf ring opening steps, similarly to the action of mineral acids [22].

By means of NMR experiments, we found that both $WOCl_4$ and **2**, when allowed to contact with limited amounts of thf in a chlorinated solvent, afforded **3**. This indicates that **2** is an intermediate along the formation of **3** (Scheme 1). Moreover, the presence of $Cl(CH_2)_4O(CH_2)_4Cl$ and $Cl(CH_2)_4Cl$ in dichloromethane mixtures (thf/W ratio = ca. 4 to 20) was pointed out.
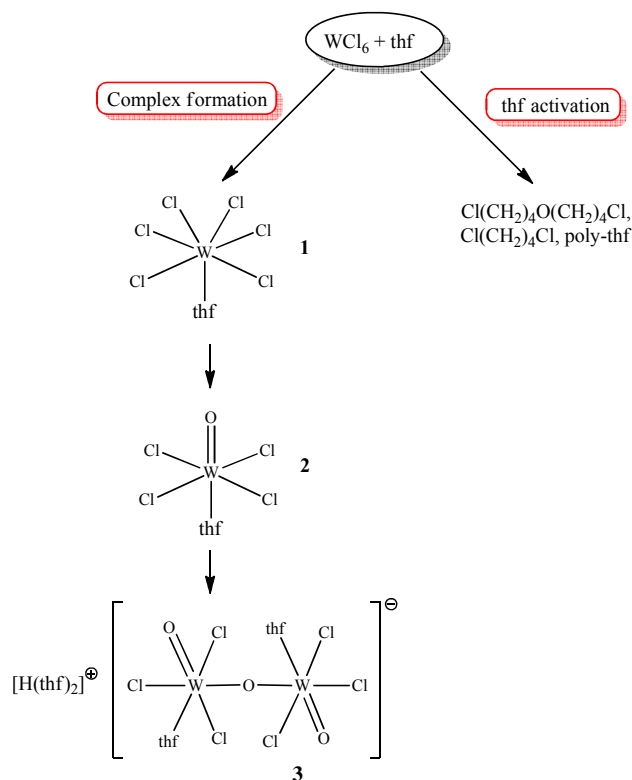
Scheme 1. Detected products from the reactions of WCl$_6$ with thf under different molar ratios.

The ether Cl(CH$_2$)$_4$O(CH$_2$)$_4$Cl is presumably the result of coupling of two thf units mediated by a tungsten centre, and may be involved in the formation of oxo-bridged complexes like **3**. Accordingly, NMR and EPR analyses on an aliquot of a thf solution of WCl$_6$ (thf/W ratio = 10) indicated the presence of **3** (traces), Cl(CH$_2$)$_4$O(CH$_2$)$_4$Cl and Cl(CH$_2$)$_4$Cl (the solution was diluted with CD$_2$Cl$_2$ in order to perform NMR analysis). In other words, the formation of these products, especially the organic ones, seems to accompany the polymerization process, and not to be restrained to the use of dichloromethane.

The ratio of Cl(CH$_2$)$_4$O(CH$_2$)$_4$Cl with respect to Cl(CH$_2$)$_4$Cl increased on increasing the thf/W ratio and was found to be higher in a reaction solution maintained at 0 °C. This fact suggests that the higher thf conversion obtained at 0 °C (run C, Table 1) might be related to the favorable formation of oxo-bridged complexes (as indirectly indicated by the higher

relative amount of the pseudo-dimer Cl(CH$_2$)$_4$O(CH$_2$)$_4$Cl), working as active catalytic (initiating) species (see above). On the other hand, while a higher conversion at lower temperature (compare run A and C) is typical of a cationic polymerization mechanism with low rate of termination reactions, the broad polydispersity of the polymer from run C (Table 1), with distinct low molecular weight fractions resulting in an average molecular weight lower than that from run A, is indicative of concurrent chain transfer to monomer. It is worth pointing out that the high conversion in run C, along with the formation of a fraction with molecular weight well over 100 kD (see Figure 1), led to a highly viscous, solid-like material, possibly promoting side reactions (e.g. the reaction of a propagating cationic chain end with one of the metal complexes).

The presence of low molecular weight poly(thf) fractions in run B (Table 1), performed under the same conditions as in run A but for a longer reaction time, is most probably the result of some uncontrolled side reactions.

2.2. Reactivity of WCl$_6$ with 2-methoxyethanol.

The treatment of a suspension of WCl$_6$ in CH$_2$Cl$_2$ with one equivalent of 2-methoxyethanol caused the formation of a light-red solution. Thus the compound (WOCl$_4$)$_2$(μ-κ^2-1,4-dioxane), **4**, was isolated in low amount by a crystallization procedure; the yield of **4** could be raised up to 20% by allowing WCl$_6$ to react with 2-methoxyethanol in 1:2 molar ratio. Compound **4** was characterized by elemental analysis, IR [14] and ^{1}H NMR spectroscopy. The IR spectrum (in the solid state) displays a diagnostic, intense absorption at 1003 cm^{-1}, ascribable to the [W=O] moiety [14]. Moreover, the X-ray molecular structure has been determined: a view of the structure is shown in Figure 8, while relevant bonding parameters are reported in Table 3.

13
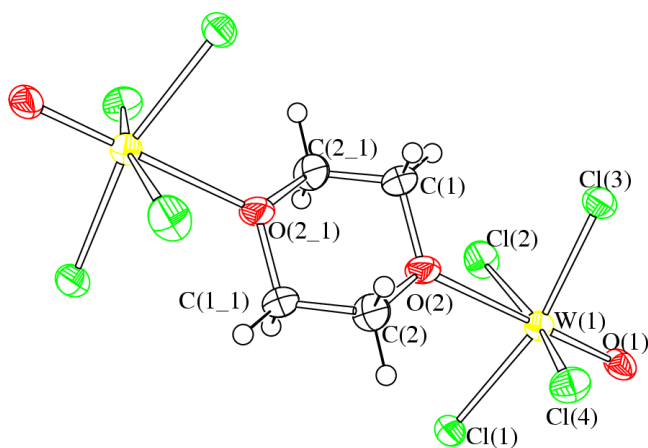
Figure 8. ORTEP representation of the content of the asymmetric unit of the unit cell of $(WOCl_4)_2(\mu-\kappa^2$-1,4-dioxane), **4**, with key atoms labeled. Displacement ellipsoids are at the 50% probability level.

Table 3. Main bond distances (Å) and angles (°) of **4**.

C(1)–O(2)	1.461(11)	C(2)–O(2)	1.471(11)
C(1)–C(2_1)	1.454(15)	W(1)–O(1)	1.692(7)
W(1)–O(2)	2.353(7)	W(1)–Cl(1)	2.307(2)
W(1)–Cl(2)	2.289(3)	W(1)–Cl(3)	2.305(2)
W(1)-Cl(4)	2.292(2)		
O(1)–W(1)–O(2)	178.7(3)	Cl(1)–W(1)–Cl(3)	163.85(9)
Cl(2)–W(1)–Cl(4)	163.62(10)	W(1)–O(2)–C(1)	125.4(6)
W(1)–O(2)–C(2)	125.5(6)	C(1)–O(2)–C(2)	107.1(8)
O(2)–C(1)–C(2_1)	110.4(9)	O(2)–C(2)–C(1_1)	110.1(9)

Compound **4** is composed by two WOCl$_4$ moieties bonded to the O-atoms of one 1,4-dioxane molecule. The molecule is located on an inversion center positioned in the center of the 1,4-dioxane ligand. The two symmetry related W-centers display a distorted octahedral geometry, with the tungsten atom moved 0.325 Å apart from the least squares plane described by the chloride ligands towards the O(1) oxo-ligand. This is a consequence of the double bond character of W(1)−O(1) [1.692(7) Å], compared to the purely dative W(1)−O(2) [2.353(7) Å] single bond. The 1,4-dioxane ligand is *trans* to the oxo-ligand, as previously found in other WOCl$_4$L complexes (L = neutral ligand) [2b,c, 3a, 6a, 23]. The structure of **4** is closely related to that of the analogous W(V) dinuclear complex [(WOCl$_4$)$_2$(μ-κ^2-1,4-dioxane)]$^{2-}$, previously reported in the literature [23a]. The geometry around the W centers is the same despite the different oxidation states, and also the W=O distances are quite similar [1.676 Å in

14

the W(V) compound, 1.692(7) Å in the W(VI) complex **4**]. Conversely, the W−O and W−Cl

contacts are longer in the W(V) complex [W−O 2.423 Å; W−Cl 2.362-2.386 Å] compared to

4 [W−O 2.353(7) Å; W−Cl 2.289(3)-2.307(2) Å].

The synthesis of **4** from WCl_6/$MeOCH_2CH_2OH$ indicates that activation of the 2-

methoxyethanol reagent takes place in the course of the reaction. More precisely, the cleavage

of C−O and O−H bonds appears to be operative followed by the formation of new C−O

bonds. In order to investigate this point, and to identify all the products of the reaction, we

allowed WCl_6 to react in the presence of two equivalents of 2-methoxyethanol in CD_2Cl_2 in a

sealed NMR tube. When the tube was opened, evolution of HCl was detected by means of a

silver chloride precipitation test (see Experimental).

NMR analysis allowed to identify the following compounds: **4**, $WCl_5(OCH_2CH_2OMe)$,

$Cl(CH_2)_2Cl$, 1,2-dimethoxyethane (dme), MeCl and some unreacted $MeOCH_2CH_2OH$

(approximate ratio 3:10:5:2:1:5), see Scheme 2. EPR analysis carried out on the same reaction

mixture evidenced the presence of paramagnetic W-species in traces only, thus suggesting

that the main reaction routes do not include W(VI) reduction.
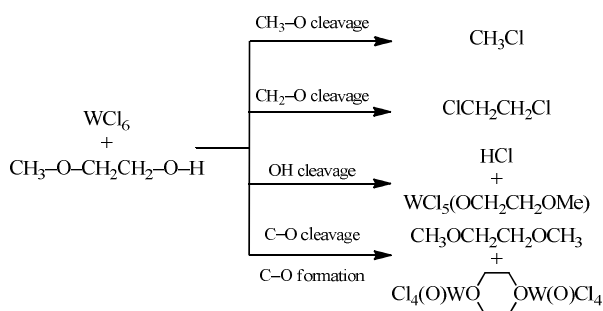
Scheme 2. Compounds identified in the mixture obtained from the reaction WCl_6 with $MeOCH_2CH_2OH$.

In agreement with the NMR outcomes, the chloride alkoxide complex $WCl_5(OCH_2CH_2OMe)$,

5 [6b], is the prevalent product of the reaction between WCl_6 and 2-methoxyethanol. The

formation of **5** and HCl appears to be the result of WCl_6 alcoholysis by 2-methoxyethanol.

Otherwise, the detection of $Cl(CH_2)_2Cl$ and $MeCl$, as well as the isolation of **4**, indicate that the breaking of both the $CH_3-O/H-O$ and $O-CH_2$ bonds in $CH_3OCH_2CH_2OH$ is occurring to some extent. Some of the produced fragments may be combined to generate dme and dioxane, this latter found in **4** (Scheme 3).
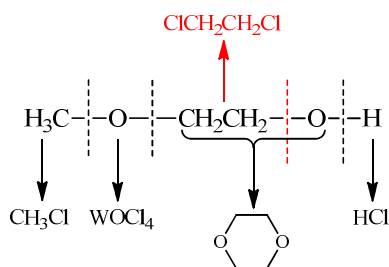
Scheme 3. Bond cleavage and formation in the reaction of WCl_6 with $MeOCH_2CH_2OH$.

We saw that heating a mixture of WCl_6 and 2-methoxyethanol, in $CDCl_3$ in a sealed NMR tube, at ca. 70 °C for 3 h, did not lead to a significant change in the composition of the final mixture.

3. Conclusions

Some metal intermediates and organic side products have been identified along the WCl_6 promoted polymerization reaction of tetrahydrofuran. In particular, ionic complexes containing oxo-bridged dinuclear anions might play some role in the growth of the polymer chain. We have elucidated also the outcome of the reaction of WCl_6 with an alkoxy-ether, i.e. 2-methoxyethanol. The prevalent product is a W(V) chloride alkoxide complex, as expected in view of the presence of the alcoholic function within the organic reactant. However additional pathways have been observed, consisting in the multiple cleavage of C−O bonds and also the C−O coupling of fragments. The latter outcome has been unambiguously evidenced by the X-ray characterization of a dioxane complex, and is not common in the context of the reactions of high valent transition metal chlorides with molecules containing

16

one or more oxygen functionalities, these reactions being usually limited to the fragmentation of the organic substrate.

4. Experimental

4.1. General procedures

Warning! the metal products reported in this paper are highly moisture-sensitive, thus rigorously anhydrous conditions were required for the reaction and crystallization procedures. The reaction vessels were oven dried at 140°C prior to use, evacuated (10^{-2} mmHg) and then filled with argon. WCl_6 was purchased from Strem (99.9% purity) and stored in sealed glass tubes under argon atmosphere. $WOCl_4$ was prepared according to the literature procedure [24]. Once isolated, the metal products were conserved in sealed glass tubes under argon. The organic reactants were commercial products (Sigma Aldrich) stored under argon atmosphere as received. Solvents (Sigma Aldrich) were distilled from appropriate drying agents before use. Infrared spectra were recorded at 298 K on a FT IR-Perkin Elmer Spectrometer, equipped with a UATR sampling accessory. NMR spectra were recorded at 298 K on a Bruker Avance II DRX400 instrument equipped with a BBFO broadband probe. The chemical shifts for ^{1}H and ^{13}C were referenced to the non-deuterated aliquot of the solvent. The spectra were fully assigned *via* [1]H,[13]C correlation measured through *gs*-HSQC and *gs*-HMBC experiments [25]. EPR spectra were recorded at 298 K on a Varian (Palo Alto, CA, USA) E112 spectrometer operating at X band, equipped with a Varian E257 temperature control unit and interfaced to IPC 610/P566C industrial grade Advantech computer, using acquisition board [26] and software package especially designed for EPR experiments [27]. Experimental EPR spectra were simulated by the WINSIM 32 program [28]. Conductivity measurements were carried out on CH_2Cl_2 solutions with Eutech Con 700 Instrument (cell constant = 1.0 cm^{-1}) [29].

Carbon and hydrogen analyses were performed on Carlo Erba mod. 1106 instrument. The chloride content was determined by the Mohr method [30] on solutions prepared by dissolution of the solid in aqueous KOH at boiling temperature, followed by cooling to room temperature and addition of HNO_3 up to neutralization.

SEC analyses were performed with a Jasco PLUS system consisting of a PU-2089 pump, CO-2063 oven set at 35 °C fitted with two PL-Gel Mixed D columns, RI-2031 differential refractometer and UV-2077 multichannel diode array UV detector. Column calibration was performed with narrow distribution poly(styrene) standards (233, 83, 23.8, 4.85 kg·mol^{-1}, Polymer Laboratories). A 40 mg/mL solution of the polymer in thf was filtered through a 0.2 μm membrane syringe filter, then 20 μL was injected and eluted at 1 mL/min flow rate with the same solvent.

4.1. Synthesis of poly-tetrahydrofuran.

General procedure: WCl_6 was added to thf in a thermostated Schlenk tube (approximate thf/W molar ratio = 2×10^2). The solution was allowed to react for a variable time. The final mixture was treated with H_2O (50 mL), and then with MeOH (50 mL), before being set aside for 3 d. The resulting solid was separated and extracted with $CHCl_3$ (100 mL). The pale yellow solution was filtered and then the solvent was removed in vacuo. The following conditions refer to Table 1.

Run A) From WCl_6 (316 mg, 0.796 mmol) and thf (12.6 mL, 155 mmol), T = 20 °C, time = 8 h. Dark green - blue solid, yield = 4.0 g (36%). ^{1}H NMR ($CDCl_3$): δ = 3.39 (m, 2 H, OCH_2), 1.59 ppm (m, 2 H, CH_2).

Run B) From WCl_6 (320 mg, 0.806 mmol) and thf (12.8 mL, 157 mmol), T = 20 °C, time = 18 h. Dark blue solid, yield = 1.9 g (17%). ^{1}H NMR ($CDCl_3$): δ = 3.37 (m, 2 H, OCH_2), 1.62 ppm (m, 2 H, CH_2).

Run C) From WCl_6 (334 mg, 0.841 mmol) and thf (13.4 mL, 165 mmol), T = 0 °C, time = 8 h. Dark green solid, yield = 8.3 g (70%). ^1H NMR ($CDCl_3$): δ = 3.39 (m, 2 H, OCH_2), 1.60 ppm (m, 2 H, CH_2).

4.2. 1:1 reaction of WCl_6 with thf: synthesis and isolation of $WOCl_4(thf)$, 2.

A mixture of WCl_6 (0.350 g, 0.883 mmol) and CH_2Cl_2 (15 mL) was treated with thf (0.150 mL, 1.85 mmol). The resulting mixture was stirred at room temperature for 24 hours. Then the volatile materials were removed in vacuo; the residue was washed with pentane (2 x 20 mL) and dried in vacuo. Compound **2** was obtained as a highly moisture sensitive, dark-yellow powder. Yield 0.300 g, 82%. Anal. Calcd for $C_4H_8Cl_4O_2W$: C, 11.61; H, 7.73; Cl, 34.27. Found: C, 11.75; H, 7.68; Cl, 34.03. IR (solid state): 2982w, 2903w, 1671w, 1453w, 1362w, 1345w, 1261w-m, 1173w, 1070w-br, 999s ($v_{W=O}$), 960w-m, 882m, 824vs-sh, 795vs, 766vs-sh, 671s cm$^-$ ^{1}. ^1H NMR (CD_2Cl_2): δ = 4.62 (m, 4 H, OCH_2), 2.19 ppm (m, 4 H, CH_2). $^{13}C\{^1H\}$ NMR (CD_2Cl_2): δ = 74.6 (OCH_2), 26.5 ppm (CH_2).

Compound **2** was isolated in ca. 85% yield by the reaction of $WOCl_4$ (0.280 g, 0.820 mmol) with thf (0.830 mmol), in CH_2Cl_2 (15 mL) at room temperature. The reaction mixture was eliminated of the volatile materials (reaction time ca. 36 h), then the yellow residue was washed with pentane (20 mL) and dried in vacuo.

4.3. Reactions of WCl_6, $WOCl_4$ and 2 with thf.

4.3.1. Synthesis and isolation of $[(thf)_2(\mu-H)][\{WOCl_3(thf)\}_2(\mu-O)]$, 3. A suspension of WCl_6 (0.380 g, 0.958 mmol) in CH_2Cl_2 (10 mL) was treated with thf (0.310 mL, 3.82 mmol). The mixture was stirred at room temperature for 4 d. Then the volatile materials were removed from the bright-green solution, and the resulting residue was washed with hexane (2 x 30 mL). Compound **3** was obtained as green crystals from a dichloromethane solution layered with

heptane, and stored at −30 °C. Yield 0.088 g, 20%. Anal. Calcd for $C_{16}H_{33}Cl_6O_7W_2$: C, 20.94; H, 3.62; Cl, 23.18. Found: C, 21.08; H, 3.53; Cl, 22.96. IR (solid state): 2980w-m, 2903w-m, 1514m, 1445m, 1403m, 1341w, 1298w, 1187br-m, 1043m, 1014m-s, 983vs ($\nu_{W=O}$), 916m, 854s, 770s (ν_{W-O-W}), 673m-s cm^{-1}. EPR (CH_2Cl_2): $g_{iso} = 1.77461$, line width = 94.48 G.

Few crystals of **3** were obtained also from the reaction of $WOCl_4$ (0.190 g, 0.556 mmol) with thf (0.138 mL, 1.70 mmol) in CH_2Cl_2 (10 mL). The reaction solution was layered with hexane and stored at −30 °C.

4.3.2. Conductivity measurements.

WCl_6 (0.530 g, 1.34 mmol) was added to thf (20 mL, 247 mmol). Immediate formation of a yellow solution took place ($\Lambda_M = 0.3$ S·cm^2·mol^{-1}). The solution turned red ($\Lambda_M = 1.3$ S·cm^2·mol^{-1}), and then green ($\Lambda_M = 5.7$ S·cm^2·mol^{-1}) and dark-green ($\Lambda_M = 5.9$ S·cm^2·mol^{-1}) in ca. 1 h. Afterwards, the medium became too viscous for further analyses.

4.4. Reaction of WCl_6 with 2-methoxyethanol: synthesis and isolation of $(WOCl_4)_2(\mu-\kappa^2-1,4-$dioxane), 4. WCl_6 (0.350 g, 0.883 mmol) was allowed to react with 2-methoxyethanol (0.142 mL, 1.80 mmol) in CH_2Cl_2 (20 mL). The mixture was stirred for 18 h at room temperature, then it was filtrated in order to remove some solid. The resulting light-red solution was concentrated up to ca. 5 mL, layered with hexane and stored at −30 °C for one week. A crop of orange-red crystals of **4** were collected. Yield: 0.068 g, 20%. Anal. Calcd for $C_4H_8Cl_8O_4W_2$: C, 6.23; H, 1.05; Cl, 36.77. Found: C, 6.12; H, 1.08; Cl, 36.65. IR (solid state): $\nu = 1448w$, 1433w, 1377w, 1295w, 1259w-m, 1096w, 1058m, 1038w, 1003s (W=O), 841vs, 814m, 784vs, 764vs cm^{-1}. ^{1}H NMR (CD_2Cl_2): $\delta = 3.85$ (br) ppm.

4.5. NMR studies.

4.5.1. Reactions of W chlorides with thf.

General procedure: The tungsten reactant, CD_2Cl_2 (0.70 mL) and a variable amount of thf were introduced into a NMR tube in the order given. Hence the tube was sealed, briefly shaken in order to homogenize the content and stored at room temperature for two weeks. ^{1}H and ^{13}C NMR analyses were carried out subsequently.

a) From WCl_6 (0.110 g, 0.277 mmol) and thf (0.044 mL, 0.54 mmol). T = 20 °C, time = 72 h. NMR analysis: **2** and $Cl(CH_2)_4Cl$ (ratio 9:10).

b) From $WOCl_4$ (0.090 g, 0.263 mmol) and thf (0.020 mL, 0.25 mmol). T = 20 °C, time = 72 h. NMR analysis: **2**.

c) From WCl_6 (0.140 g, 0.353 mmol) and thf (0.115 mL, 1.42 mmol). T = 20 °C, time = 96 h. NMR analysis: $Cl(CH_2)_4O(CH_2)_4Cl$ and $Cl(CH_2)_4Cl$ (prevalent), 1,3-butadiene (traces).

d) From WCl_6 (0.140 g, 0.353 mmol) and thf (0.115 mL, 1.42 mmol). T = 0 °C, time = 10 d. NMR analysis: $Cl(CH_2)_4O(CH_2)_4Cl$ (prevalent) and $Cl(CH_2)_4Cl$.

e) From $WOCl_4$ (0.120 g, 0.351 mmol) and thf (0.086 mL, 1.06 mmol). T = 20 °C, time = 96 h. NMR analysis: $Cl(CH_2)_4O(CH_2)_4Cl$ and $Cl(CH_2)_4Cl$ (prevalent).

f) From WCl_6 (0.090 g, 0.227 mmol) and thf (0.380 mL, 4.68 mmol). T = 20 °C, time = 96 h. ^{13}C NMR analysis allowed to identify poly-thf, $Cl(CH_2)_4O(CH_2)_4Cl$ and $Cl(CH_2)_4Cl$.

*4.5.2 Reaction of WCl_6 with 2-methoxyethanol: identification of $WCl_5(OCH_2CH_2OMe)$, **5**, $Cl(CH_2)_2Cl$, dme and MeCl.*

WCl_6 (0.130 g, 0.328 mmol), CD_2Cl_2 (0.70 mL) and 2-methoxyethanol (0.025 mL, 0.317 mmol) were introduced into a NMR tube in the order given. The tube was sealed, and briefly shaken in order to homogenize the content. NMR analysis was carried out after one week. ^{1}H NMR (CD_2Cl_2): δ = 5.71 (br, OCH_2, **5**), 4.26 (br, CH_2, **5**), 4.00 (s, OMe, **5**), 3.93 (br, **4**), 3.74 (s, $ClCH_2CH_2Cl$), 3.61 (s, CH_2, $MeOCH_2CH_2OH$), 3.57 (br, CH_2, dme and $MeOCH_2CH_2OH$), 3.43 (s, CH_3, dme), 3.41 (s, CH_3, $MeOCH_2CH_2OH$), 3.06 (s, MeCl) ppm. Ratio

4:5:Cl(CH$_2$)$_2$Cl:dme:MeCl:MeOCH$_2$CH$_2$OH = ca. 3:10:5:2:1:5. ^{13}C{^{1}H} NMR (CD$_2$Cl$_2$): δ = 79.4 (CH$_2$, **5**), 75.8 (CH$_2$, **5**), 72.8 (CH$_2$, dme), 63.2 (OMe, **5**), 59.1 (CH$_3$, dme), 43.6 (ClCH$_2$CH$_2$Cl) ppm.

When the tube was opened, gas release occurred. This gas (HCl) was bubbled into a concentrated aqueous solution of AgNO$_3$, thus precipitation of a white solid (AgCl) occurred.

4.6. X-ray Crystallography.

Crystal data and collection details for **3** and **4** are listed in Table 4. The diffraction experiments were carried out on Bruker APEX II diffractometer equipped with CCD detector and using Mo-Kα radiation. Data were corrected for Lorentz polarization and absorption effects (empirical absorption correction SADABS) [31]. The structures were solved by direct methods and refined by full-matrix least-squares based on all data using F^2 [31]. Hydrogen atoms of **3** were fixed at calculated positions and refined by a riding model, except H(7) bonded to O(7) which was located in the Fourier map and refined using the 1.2-fold *U*-value of the parent atom. The O(7)–H(7) distance has been restrained to 0.9 Å (s.u. 0.02). Similar *U* restraints [SIMU line in SHELXL; s.u. 0.01] were applied to all the C-atoms of **3**. The crystals of **3** are racemically twinned with refined absolute structure parameter 0.383(14). All non-hydrogen atoms of **4** were refined with anisotropic displacement parameters, while H-atoms were placed in calculated positions and treated isotropically using the 1.2 fold U_{iso} value of the parent atom. The asymmetric unit of the unit cell of **4** contains half of a molecule located on an inversion center. A high residual electron density remains after refinement at 0.91 Å from W(1) due to absorption effects: an ALERT A due to high residual electron density values is present in the CHECKCIF; this maximum is located close to the W-atom and it is a series termination error which is common with heavy atoms such as W.

Table 4. Crystal data and details of the structure refinement for **3** and **4**.

	3	**4**
Formula	$C_{16}H_{33}Cl_6O_7W_2$	$C_4H_8Cl_8O_4W_2$
Fw	917.82	771.40
λ, Å	0.71073	0.71073
Temperature, K	100(2)	100(2)
Crystal system	Monoclinic	Orthorhombic
Space group	Pn	Pbca
a, Å	10.023(2)	10.7436(15)
b, Å	11.337(2)	10.7206(15)
c, Å	12.651(3)	14.069(2)
β, °	111.501(2)	===
Cell volume, Å^3	1337.4(5)	1620.5(4)
Z	2	4
D_c, g cm^{-3}	2.279	3.162
μ, mm^{-1}	9.227	15.503
F(000)	1752	1392
Crystal size	0.16×0.12×0.11	0.16×0.14×0.12
θ limits, °	1.80–25.02	2.90–25.99
Reflections collected	12116	15241
Independent reflections	4701 [R_{int} = 0.0474]	1600 [R_{int} = 0.0569]
Data / restraints / parameters	4701 / 76 / 284	1600/ 0 / 82
Goodness of fit on F^2	1.040	1.076
R1 (I > 2σ(I))	0.0367	0.0380
wR2 (all data)	0.0785	0.0987
Largest diff. peak and hole, e.Å^{-3}	1.233 / -1.481	6.082 / –1.625

4.7. Computational studies.

The computational geometry optimizations were carried out without symmetry constrains, using the range-separated DFT functional ωB97X [32] in combination with the split-valence polarized basis set of Ahlrichs and Weigend, with ECP on the metal centre [33]. The "unrestricted" formalism was applied to compounds with unpaired electrons, and the lack of spin contamination was verified by comparing the computed $<S^2>$ values with the theoretical ones. The stationary points were characterized by IR simulations (harmonic approximation), from which zero-point vibrational energies and thermal corrections (T = 298.15 K) were obtained [34]. The C-PCM implicit solvation model (ε = 9.08) was added to ωB97X calculations [35]. Bond orders were estimated on the basis of Mayer's approach [36]. The software used were Gaussian '09 [37] and Multiwfn version 3.3.8 [38].

Supporting Information. CCDC contain the supplementary crystallographic data for the X-ray study reported in this paper. CCDC 1484850 (**3**) and 1476772 (**4**). For ESI and crystallographic data in CIF or other electronic format see DOI: XXXXXXX

References

1   (a) M. A. Zolfigol, A. R. Moosavi-Zare, P. Arghavani-Hadi, A. Zare, V. Khakyzadeh, G. Darvishi, RSC Advances 2 (2012) 3618–3620.

(b) Q. Guo, T. Miyaji, R. Hara, B. Shen, T. Takahashi, Tetrahedron 58 (2002) 7327-7334.

(c) Q. Guo, T. Miyaji, G. Gao, R. Hara, T. Takahashi, Chem. Commun. (2001) 1018-1019.

(d) H. Firouzabadi, N. Iranpoor, B. Karimi, Synlett (1998) 739-740.

2   a) M. Bortoluzzi, F. Marchetti, M. G. Murrali, G. Pampaloni, S. Zacchini, Dalton Trans. 44 (2015) 8729-8738.

b) M. Bortoluzzi, F. Guarra, F. Marchetti, G. Pampaloni, S. Zacchini, Polyhedron 99 (2015) 141–146.

c) S. Dolci, F. Marchetti, G. Pampaloni, S. Zacchini, Dalton Trans. 42 (2013) 5635-5648.

3   a) P. D. W. Boyd, M. G. Glenny, C. E. F. Rickard, A. J. Nielson, Polyhedron 30 (2011) 632-637.

b) H. Balcar, A. Dosedlová, B. Matyska, J. Mol. Catal. 41 (1987) 367-374.

c) H. Balcar, A. Dosedlová, B. Matyska, Coll. Czech. Chem. Commun. 51 (1986) 753-762.

4   a) M. Bortoluzzi, F. Marchetti, G. Pampaloni, S. Zacchini, Chem. Commun. 51 (2015) 1323-1325.

b) H. Tsurugi, H. Tanahashi, H. Nishiyama, W. Fegler, T. Saito, A. Sauer, J. Okuda, K. Mashima, J. Am. Chem. Soc. 135 (2013) 5986-5989.

c) A. J. Nielson, P. A. Hunt, C. E. F. Rickard, P. Schwerdtfeger, J. Chem. Soc., Dalton Trans. (1997) 3311–3317.

d) O. J. Klejnot, Inorg. Chem. 4 (1965) 1668-1670.

5   U. Jayarathne, J. T. Mague, J. P. Donahue, Polyhedron 58 (2013) 13-17.

6   (a) M. Bortoluzzi, F. Marchetti, G. Pampaloni, S. Zacchini, Eur. J. Inorg. Chem. (2016) 3169-3177.

(b) S. Dolci, F. Marchetti, G. Pampaloni, S. Zacchini, Dalton Trans. 39 (2010) 5367-5376.

7   L. Favero, F. Marchetti, G. Pampaloni, S. Zacchini, Dalton Trans. 43 (2014) 495-504.

8   F. Marchetti, G. Pampaloni, S. Zacchini, Dalton Trans. (2008) 7026-7035.

9   (a) B. J. Brisdon, M. F. Mahon and C. C. Rainford, J. Chem. Soc., Dalton Trans. (1998) 3295–3299.

(b) Y. Takegami, T. Ueno and R. Hirai, Bull. Chem. Soc. Jpn. 38 (1965) 1222.

10   W. Levason, C. A. Mcauliffe And F. P. Mccullough Jr., Inorg. Chem. 16 (1977) 2911-2916.

11   (a) F. Marchetti, G. Pampaloni, S. Zacchini, Polyhedron 85 (2015) 369-375.

(b) C. Limberg, R. Boese, B. Schiemenz, J. Chem. Soc., Dalton Trans. (1997) 1633–1637.

(c) F. Quignard, M. Leconte, J.-M. Basset, L.-Y. Hsu, J. J. Alexander, S. G. Shore, Inorg. Chem. 26 (1987) 4212-4211.

(d) O. J. Klejnot, Inorg. Chem. 4 (1965) 1668-1670.

(e) D. C. Bradley, R. K. Multani, W. Wardla, J. Chem. Soc. (1958) 4647-4651.

12   J. A. Emerson, D. T. W. Toolan, J. R. Howse, E. M. Furst, T. H. Epps III, Macromolecules 46 (2013) 6533–6540.

13   A. Decken, C. Knapp, G. B. Nikiforov, J. Passmore, J. M. Rautiainen, X. Wang, X. Zeng, Chem. Eur. J. 15 (2009) 6504.

14   G. W. A. Fowles, J. L. Frost, J. Chem. Soc. A (1967) 671-675.

15   a) B. Siewert, U. Müller, Z. Anorg. Allg. Chem. 609 (1992) 77-81. (b) S. Buth, B. Neumüller, K. Dehnicke, Z. Kristallogr. 208 (1993) 326-329

16   G. Kirsten, H. Görls, W. Seidel, Z. Anorg. Allg. Chem. 624 (1998) 887-891.

17   (a) J. Pietikäinen, A. Maaninen, R. S. Laitinen, R. Oilunkaniemi, J. Valkonen, Polyhedron 21 (2002) 1089-1095.

(b) D. Stasko, S. P. Hoffmann, K.-C. Kim, N. L. P. Fackler, A. S. Larsen, T. Drovetskaya, F. S. Tham, C. A. Reed, C. E. F. Rickard, P. D. W. Boyd, E. S. Stoyanov, J. Am. Chem. Soc. 124 (2002) 13869-13876.

(c) I. Krossing, A. Reisinger, Eur. J. Inorg. Chem. (2005) 1979-1989

18   (a) W. Willing, F. Schmock, U. Muller, K. Dehnicke, Z. Anorg. Allg. Chem. 532 (1986) 137-144.

(b) Y. Jeannin, J. –P. Launay, J. Livage, A. Nel, Inorg. Chem. 17 (1978) 374-378.

19   (a) T. Glowiak, M. Sabat, B. Jezowska-Trzebiatowska, Acta Crystallogr., Sect. B 31 (1975) 1783-1784.

(b) P. M. Smith, Diss. Abstr. Int. B. 32 (1972) 5136.

20   M. Kersting, C. Friebel, K. Dehnicke, M. Krestel, R. Allmann, Z. Anorg. Allg. Chem. 563 (1988) 70-78.

21   P. B. Arimondo, F. Calderazzo, R. Hiemeyer, C. Maichle-Mössmer, F. Marchetti, G. Pampaloni, J. Strähle, Inorg. Chem. 37 (1998) 5507-5511.

22   a) H. Meerwein, D. Delfs, H. Morschel, Angew. Chem. 72 (1960) 927–1006.

b) P. Dreyfuss, M. P. Dreyfuss, Adv. Polym. Sci. 4 (1967) 528–590, and references therein.

23   (a) A. Okrut, C. Feldmann, Z. Anorg. Allg. Chem. 633 (2007) 2144-2146.

(b) V. S. Sergienko, V. L. Abramenko, A.B. Ilyukhin, Russ. J. Inorg. Chem. 42 (1997) 847-852.

(d) I.W. Bassi, R. Scordamaglia, J. Organomet. Chem. 99 (1975) 127-134.

24   V. C. Gibson, T. P. Kee, A. Shaw, Polyhedron 9 (1990) 2293-2298.

25   W. Willker, D. Leibfritz, R. Kerssebaum, W. Bermel, Magn. Reson. Chem. 31 (1993) 287-292.

26   R. Ambrosetti, D. Ricci, Rev. Sci. Instrum. 62 (1991) 2281-2287.

27   C. Pinzino, C. Forte, EPR-ENDOR, ICQEM-CNR Rome, Italy (1992).

28   D. R. Duling, J. Magn. Reson. B 104 (1994) 105-110.

29   (a) A. Jutand, Eur. J. Inorg. Chem. (2003) 2017-2040.

(b) W. J. Geary, Coord. Chem. Rev. 7 (1971) 81-122.

30   D. A. Skoog, D. M. West, F. J. Holler, Fundamentals of Analytical Chemistry, 7th Edition, Thomson Learning, Inc, USA (1996).

31   G. M. Sheldrick, SHELX97-Program for the refinement of Crystal Structure, University of Göttingen, Göttingen ,Germany (1997).

32   (a) Y. Minenkov, Å. Singstad, G. Occhipinti, V. R. Jensen, Dalton Trans. 41 (2012) 5526-5541.

(b) J.-D. Chai, M. Head-Gordon, Phys. Chem. Chem. Phys. 10 (2008) 6615-6620.

(c) I. C. Gerber, J. G. Ángyán, Chem. Phys. Lett. 415 (2005) 100-105.

33   (a) F. Weigend, R. Ahlrichs, Phys. Chem. Chem. Phys. 7 (2005) 3297-3305.

(b) D. Andrae, U. Haeussermann, M. Dolg, H. Stoll, H. Preuss, Theor. Chim. Acta 77 (1990) 123-141.

34   C. J. Cramer, Essentials of Computational Chemistry, 2nd Edition, Wiley, Chichester (2004).

35   (a) M. Cossi, N. Rega, G. Scalmani, V. Barone, J. Comput. Chem. 24 (2003) 669–681.

      (b) V. Barone, M. Cossi, J. Phys. Chem. A 102 (1998) 1995–2001.

36   (a) A. J. Bridgeman, G. Cavigliasso, L. R. Ireland, J. Rothery, J. Chem. Soc., Dalton Trans. (2001) 2095-2018.

      (b) I. Mayer, Int. J. Quantum Chem. 26 (1984) 151-154.

37   Gaussian 09, Revision C.01, M. J. Frisch, et al., Gaussian, Inc., Wallingford CT (2010).

38   T. Lu, F. Chen, J. Comput. Chem. 33 (2012) 580-592.